Hindawi
Advances in Meteorology
Volume 2022, Article ID 6294029, 11 pages
https://doi.org/10.1155/2022/6294029

Research Article

Separating the Impact of Climate Changes and Human Activities on Vegetation Growth Based on the NDVI in China

Wenli Lai,[1,2] **Mingming Wang**,[3] **Jun Wei**,[3] **Jie Zhang**,[4] **Jiayu Song**,[4] **Haiyan Zhou**,[4] **Shuren Chou**,[5] **and Yongping Wang**[5]

[1]*College of Geography and Environmental Science, Hainan Normal University, Haikou 571158, China*
[2]*Key Laboratory of Earth Surface Processes and Environmental Change of Tropical Islands, Haikou, Hainan, China*
[3]*Power China Huadong Engineering Corporation Limited, Hangzhou 311122, China*
[4]*College of Ecology and Environment, Hainan University, Haikou 570228, China*
[5]*Space Engineering University, Beijing 101416, China*

Correspondence should be addressed to Jie Zhang; zhang_jie@hainanu.edu.cn

Received 17 November 2021; Revised 28 February 2022; Accepted 23 March 2022; Published 12 April 2022

Academic Editor: Budong Qian

Vegetation growth is affected by both climate changes and human activities. In this study, we investigated the vegetation growth response to climate change (precipitation and temperature) and human activities in nine subregions and for nine vegetation types in China from 1982 to 2015. The normalized difference vegetation index (NDVI) and the RESTREND method based on a multiple linear regression model were employed to this end. An overall increasing trend in the NDVI was observed in recent decades, and the fastest increases were identified in southern China ($Trend_{NDVI} = +0.0190$) and evergreen broad-leaved forests ($Trend_{NDVI} = +0.0152$). For >66% of China, vegetation is more sensitive to temperature and less sensitive to precipitation based on the regression coefficients. The water demand for vegetative growth increased significantly from 1999 to 2015 with global warming, especially in parts of the temperate zone. We defined a relative change in the residual trend to quantify the impact of human activities on vegetation. $RESTREND_{NDVI}$/NDVI in two periods (P1, 1982–1998 and P2, 1999–2015) markedly increased, indicating that human activities play a key role in the reversal of land degradation.

1. Introduction

Vegetation impacts the water cycle via various processes, including transpiration [1, 2], canopy interception [3, 4], and the conservation of water and soil [5–7]. In the context of climate change, precipitation and temperature are recognized as the two major climatic factors affecting the biophysical processes of vegetation [8, 9]. A warmer climate can increase the length of the growing season [10] and wetter conditions mitigate water demand stress and improve plant productivity in arid and semiarid regions [11]. Under the influence of both climate changes and human activities, the changes in vegetation have become more complicated in various climatic regions [9, 12]. With rapid economic development, ecological systems have suffered severe damage through overgrazing and land reclamation in China, for example, in the Qinghai-Tibet Plateau [13] and Inner Mongolian grasslands [14]. Moreover, rapid urbanization and population growth limit the potential growth areas for vegetation.

In 1999, the Grain for Green Project was initiated to reduce the soil erosion and improve local ecological conditions, including for the Loess Plateau, in the northern areas of Shaanxi Province [15], for the upper and middle Yangtze River in Sichuan Province [16], and the typical arid/semiarid rainfed agricultural areas in Gansu Province [17]. The Grain for Green Project has led to the conversion of ~16,000 km^2 of rainfed agriculture land in semiarid regions to grassland and forests, resulting in an ~25% increase in vegetation cover of the Loess Plateau from 1999 to 2010. The benefit of both water resource and land-use management (e.g., conservation of water and soil [5, 18], water-saving agriculture [19, 20],

and returning farmland to forests [21]) and climate change (e.g., more precipitation in arid/semiarid regions and temperature increasing in high-latitude regions [22, 23]) affects local ecological conditions. Especially entering the 21st century, human activities have played an important role in vegetation change [24, 25]. It is necessary to identify effects due to climate changes and human activities at regional scales. Two periods of 1982–1998 (before the Grain for Green Project) and 1999–2015 (after) were analyzed in this study.

With the development of remote sensing, massive amounts of data are widely employed to investigate changes in vegetation [26] and human activities [27, 28] at large scales. Since the 1980s, a series of vegetation indices have been developed using remote sensing datasets, for example, the normalized difference vegetation index (NDVI) and enhanced vegetation index (EVI), derived from infrared and near-infrared spectral bands to quantify long-term changes in vegetation growth [29, 30]. Several studies have focused on attributing the changes in vegetation using remote sensing means [9, 10]. A significant increase in the NDVI is observed in some arid and semiarid regions of China, for example, in Northwest China, due to the vegetation's enhanced sensitivity to wet conditions [31]. A decreasing trend in the EVI was detected in the Yangtze River Basin due to urbanization [9]. Based on previous studies, there is a positive relationship with warming in most parts of China; however, the response sensitivity of vegetation differed with seasons and vegetation types [32, 33].

In recent decades, a series of approaches have been developed to quantify the impact of climate changes and human activities on vegetation. The most widely used effective methods can be divided into three categories [15]: (i) regression model-based methods, (ii) biophysical model-based methods, and (iii) residual trend-based methods. The regression model-based method uses regression statistics to examine the relationship between vegetation change and climate or human-related factors. However, it is unsuitable to distinguish the complex interactions between vegetation and influencing factors (climatic and anthropogenic factors) [34]. Second, the biophysical model-based method is common; however, several physiological and ecological parameters need to be measured or calibrated and the effect of equifinality for different parameters is unavoidable in a complex system [34]. Third, as one of the most widely used methods for separating the impact of climate changes and human activities on vegetation, the residual trend-based method (RESTREND) is a robust approach. The trend in the residuals of multiple regression between climatic factors and vegetation indicators (e.g., NDVI, GPP, and NPP) can quantify the impact of human activities on vegetation.

In this study, we quantify the sensitivity of climate variables in response to vegetation growth in a warming climate across various climatic regions and different vegetation types in China. To this end, MLR and the residual trend (RESTREND) analysis method were employed to separate the impact of climate changes and human activities. The rest of the article is organized as follows: in Section 2, we describe the long-term meteorological and remote sensing datasets and statistical methods. In Section 3, we report the assessment and attribution results of long-term changes in vegetation from 1982 to 2015. We present our discussion and conclusions in Section 4 and Section 5, respectively.

2. Materials and Methods

2.1. Data Sources. GPCC datasets are recommended for hydro-meteorological model verification and water cycle studies owing to the high data quality and long-term time series. In this study, we selected the monthly precipitation GPCC datasets ($0.5^\circ \times 0.5^\circ$ longitude by latitude) covering the mainland of China from 1982 to 2015. This analysis is based on meteorological stations established before 1900, and GPCC datasets span the period from 1891 to 2016. In this study, the period from 1982 to 2015 is covered. The coincident monthly spatial resolution ($0.5^\circ \times 0.5^\circ$ longitude by latitude) and the period (1982 to 2015) air temperature datasets, and the Hadley Centre and Climatic Research Unit HadCRUT4 datasets including 3839 grid boxes were used in this study.

Semimonthly, the long-term NDVI of GIMMS NDVI3g datasets were used. GIMMS NDVI3g datasets are global vegetation index change data provided by NASA (https://ecocast.arc.nasa.gov/data/pub/gimms/3g.v1/). The dataset is preprocessed by data fusion, radiometric correction, geometric correction, bias correction, and image enhancement. It is commonly used in the study of regional and global vegetation change owing to the long time frame and homogeneous series [10, 35]. In this study, we obtained GIMMS NDVI data from January 1982 to December 2015. To minimize the influence of clouds, atmosphere, and monthly phenology, which is considered a possible source of noise, the maximum value composite method was adopted to merge the datasets from the semimonthly to monthly scale. To ensure consistent spatial resolution for precipitation, air temperature, and NDVI, we uniformly aggregated to 0.5 using the nearest-neighbor resampling method.

The land cover map for 2015 from the European Space Agency Climate Change Initiative (https://maps.elie.ucl.ac.be/CCI/) was also re-gridded to the 0.5 grid using the nearest-neighbor method and used to classify vegetation types. The nine subregions of China are shown in Figure 1(a). We reclassified the 38 land cover types into nine categories, namely croplands—CRO, evergreen broad-leaved forests—EBF, deciduous broad-leaved forests—DBF, evergreen needleleaf forests—ENF, deciduous needleleaf forests—DNF, mixed forests—MF, shrublands—SHR, grasslands—GRA, and non-vegetation regions—NOV (Figure 1(b)).

3. Methods

The linear regression equation is expressed as follows:

$$Y_t = aX_t + b + \varepsilon, \tag{1}$$

where Y_t is the dependent variable in the year t (Y is the annual series of NDVI for a given grid box), X is the independent variable (X is the annual series from 1982 to 2015

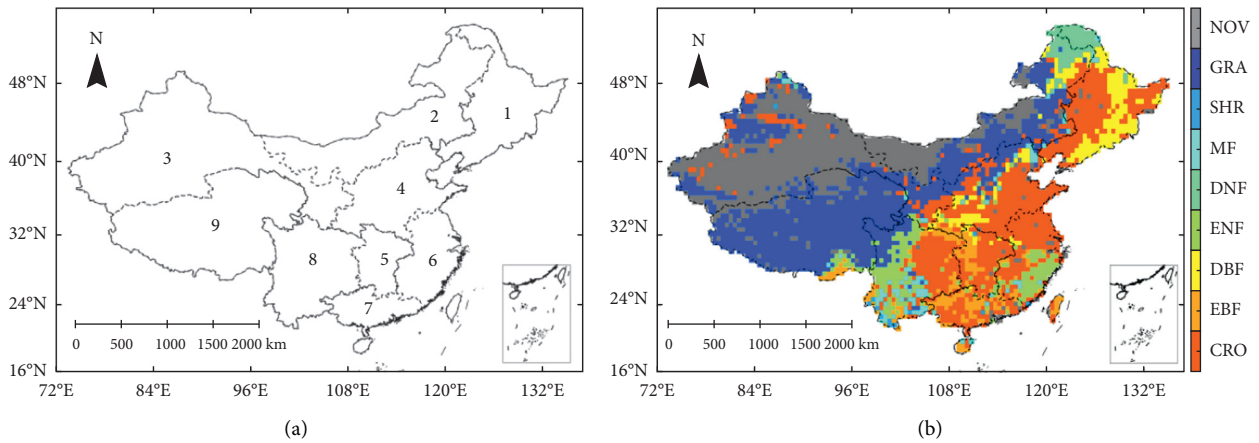

FIGURE 1: Study area covering (a) nine large subregions (1: Northeast China, 2: Inner Mongolia, 3: Northwest China, 4: North China, 5: Central China, 6: Southeast China, 7: South China, 8: Southwest China, and 9: Tibetan Plateau) with various vegetation types (CRO: croplands, EBF: evergreen broad-leaved forests, DBF: deciduous broad-leaved forests, ENF: evergreen needleleaf forests, DNF: deciduous needleleaf forests, MF: mixed forests, SHR: shrublands, GRA: grasslands, and NOV: non-vegetation regions).

for a given grid box), a and b are the slope and the intercept, respectively, and ε is the residual for the regression equation.

The slope of NDVI is given as follows:

$$\text{slope} = \frac{\text{Cov}(X, Y)}{\text{Var}(X)}. \tag{2}$$

The statistic value S of the Mann-Kendall test is defined as follows:

$$S = \sum_{i=1}^{t-1} i \sum_{j=i+1}^{t} \text{sign}\left(\text{NDVI}_i - \text{NDVI}_j\right), \tag{3}$$

where

$$\text{sign}\left(\text{NDVI}_i - \text{NDVI}_j\right) = \begin{cases} -1, & \text{if}\left(NDVI_i - NDVI_j < 0\right), \\ 0, & \text{if}\left(NDVI_i - NDVI_j = 0\right), \\ 1, & \text{if}\left(NDVI_i - NDVI_j > 0\right). \end{cases} \tag{4}$$

The variance of S is as follows:

$$\text{Var}(S) = \frac{t(t-1)(2t+5)}{18}. \tag{5}$$

The statistic Z is defined as follows:

$$Z = \begin{cases} \dfrac{(S-1)}{\sqrt{\text{Var}(S)}}, & S > 0, \\ 0, & S = 0, \\ \dfrac{(S+1)}{\sqrt{\text{Var}(S)}}, & S < 0. \end{cases} \tag{6}$$

Based on a confidence level of 0.05 using the Mann-Kendall test, if $|Z| \geq 1.96$, the statistical value of the trend is significant [36].

MLR was used to quantify the contribution of meteorological variables. In this sensitivity analysis, sunshine duration (solar radiation) was eliminated because of the multicollinearity with precipitation [9]. To compare two independent variables, we first normalized the annual series of all variables (both dependent and independent) as a dimensionless series with a large sample size ($\mu = 0$; $\sigma = 1$):

$$X_i = \frac{(x_i - \overline{x})}{\sigma(x)}, \tag{7}$$

where x is the original annual series, that is, P, T, and NDVI, and X is the dimensionless series.

The regression coefficient (hereafter as RC) obtained from the MLR is an appropriate measure for identifying a variable as being independent. The RESTREND method examines the change in residual differences between the observed and predicted annual NDVI based on the MLR model using climate variables (e.g., temperature and precipitation) as independent parameters [37]. To distinguish this influence before or after the Chinese Grain for Green program, the long-term climatic change was divided into two periods (Period 1, 1982–1998 and Period 2, 1999–2015). The annual NDVI residual trend was calculated based on MLR with the annual air temperature and precipitation. The calculation of the RESTREND method is as follows:

$$\text{NDVI} = a_1 P + a_2 T + \varepsilon, \tag{8}$$

where P is the annual precipitation, T is the annual temperature, and ε is the residual based on the MLR model.

Then the RESTREND can be quantified by linear regression:

$$\text{RESTREND} = \frac{\text{cov}(\varepsilon, \text{years})}{\text{var}(\varepsilon)}, \quad (9)$$

where *years* is a given period (1982–2015, 1982–1998, or 1999–2015) corresponding to the residual of ε.

4. Results

4.1. Detecting Vegetation Trends Using the NDVI from 1982 to 2015. By analyzing the trend in the annual NDVI from 1982 to 2015 at the grid box level (Figure 2(a)), a significant increasing trend in the vegetation (termed as "greening") was detected in most regions of China (Figure 2(a) and 2(b)). The fastest greening region was found in Central China ($\text{Trend}_{\text{NDVI}} = +0.0190 \cdot 10a^{-1}$), followed by Southwest China ($\text{Trend}_{\text{NDVI}} = +0.0165 \cdot 10a^{-1}$), South China ($\text{Trend}_{\text{NDVI}} = +0.0147 \cdot 10a^{-1}$), most of the Tibetan Plateau ($\text{Trend}_{\text{NDVI}} = +0.01067$), and North China ($\text{Trend}_{\text{NDVI}} = +0.0131 \cdot 10a^{-1}$). A small increasing vegetation trend (trend in the NDVI less than 0.01, decade^{-1}) was found in Southeast China ($\text{Trend}_{\text{NDVI}} = +0.00173 \cdot 10a^{-1}$), Inner Mongolia ($\text{Trend}_{\text{NDVI}} = +0.0013 \cdot 10a^{-1}$), and Northwest China ($\text{Trend}_{\text{NDVI}} = +0.0007$). By contrast, a decrease in the NDVI was detected at grid scales and distributed sporadically in Northeast China ($\text{Trend}_{\text{NDVI}} = -0.0087 \cdot 10a^{-1}$), Eastern Inner Mongolia, and northern Northwest China.

For different land covers (vegetation types), as shown in Figure 2(c), the fastest greening region was found in evergreen broad-leaved forests ($\text{Trend}_{\text{NDVI}} = +0.0152$), followed by croplands ($\text{Trend}_{\text{NDVI}} = +0.0127$), mixed forests ($\text{Trend}_{\text{NDVI}} = +0.0126$), shrublands ($\text{Trend}_{\text{NDVI}} = +0.0109$), and evergreen needleleaf forests ($\text{Trend}_{\text{NDVI}} = +0.0102$). A smaller increasing trend in vegetation (trend in the NDVI less than 0.01 per decade) was found in deciduous needleleaf forests ($\text{Trend}_{\text{NDVI}} = +0.0026$), deciduous broad-leaved forests ($\text{Trend}_{\text{NDVI}} = +0.0023$), grasslands ($\text{Trend}_{\text{NDVI}} = +0.0022$), and non-vegetated areas ($\text{Trend}_{\text{NDVI}} = +0.0006$).

4.2. Sensitivity Analysis for Vegetation Using MLR. To explore the sensitivity of vegetation to precipitation (indicating water stress) and temperature, a multiple regression model was designed using standardized NDVI (dependent variable) and standardized climatic variables (precipitation and temperature as independent variables) merged into an annual time series to remove the lagged response of vegetation within monthly periods.

To eliminate the interference factors in a non-vegetated area, we extracted the regression coefficient of precipitation (RC_P) and temperature (RC_T) to annual NDVI without counting the grid boxes of the non-vegetated land cover type at grid scales (Figure 3(a)). On the whole of China, 70.2% of grid boxes indicated that the vegetation is more sensitive to temperature ($|RC_P| < |RC_T|$). The contribution (regression coefficient) of precipitation to vegetation trends has a large spatial difference at grid scales, ranging from −0.60 in the north of Northeast China to +0.69 in Eastern Inner Mongolia (Figure 3(a)). The regression coefficient of temperature showed a different spatial pattern, ranging from −0.37 in the south of the Tibetan Plateau to +0.79 in the north of Central China over the same period (Figure 3(a) and 3(b)).

For the nine subregions of China, we note a significantly positive response of vegetation to precipitation (an average RC_P over +0.1) in nonhumid regions of China, for example, Inner Mongolia ($RC_P = +0.302$), North China ($RC_P = +0.270$), and Northwest China ($RC_P = +0.140$). The response of vegetation to precipitation is relatively insensitive in the other subregions (the average RC_P around zero, greater than −0.1 and less than +0.1). By contrast, the significantly positive response of vegetation to temperature (an average RCP over +0.1) was found in all subregions of China, especially in Central China ($RC_T = +0.547$), North China ($RC_T = +0.426$), the Tibetan Plateau ($RC_T = +0.438$), and South China ($RC_T = +0.399$).

Using multiple linear regression (MLR) analysis, we obtained the regression coefficient of precipitation with different land covers (vegetation types). On average, the regression coefficient of precipitation ranged from −0.205 in deciduous needleleaf forests to 0.144 in grasslands. The deciduous needleleaf forests, with a negative response to precipitation, are the most sensitive land-use type ($RC_P = -0.205$). As shown in Figure 3(b), increased precipitation also favors vegetation increases in other individual land-use types (e.g., evergreen broad-leaved forests, $RC_P = -0.017$; deciduous broad-leaved forests, $RC_P = -0.094$; evergreen needleleaf forests, $RC_P = -0.059$; shrublands, $RC_P = -0.143$). On average, the regression coefficient of temperature ranged from 0.149 in deciduous needleleaf forests to 0.405 in evergreen broad-leaved forests. Compared with the regression coefficient of precipitation, we found that the absolute value of the regression coefficient for temperature is significantly higher in most land-use types, except for deciduous needleleaf forests ($|RC_P| > |RC_T|$ in the deciduous needleleaf forests in China). This means that the response of vegetation to precipitation is significantly weaker than that of temperature, except for deciduous needleleaf forests (Figure 3(b)).

4.3. Contribution of Climate Changes and Human Activities to Interannual Variation of the NDVI in the Two Periods. With dramatic global warming occurring at global and regional scales, quantitatively determining the contribution of climate changes and human activities to the NDVI is essential for understanding the trends in vegetation change. Previous studies have highlighted that vegetation growth is relatively sensitive to climate changes (e.g., temperature and precipitation), and the influence of human activities on vegetation growth must not be ignored [9, 38]. The correlation coefficient of the MLR model (CC) mentioned in Section 3.2 can indicate the impact of climate changes on vegetation with global warming. Here, we prepared a long-term annual temperature series spanning 1982 to 2015 (Figure 4). We noted that the annual temperature slowly

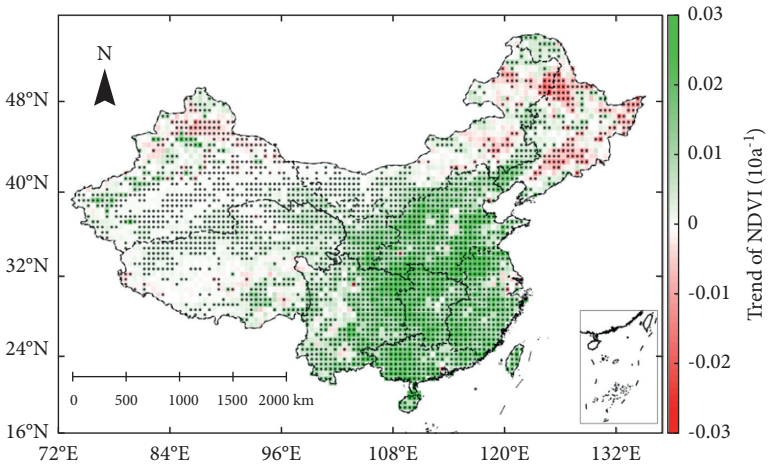

(a)

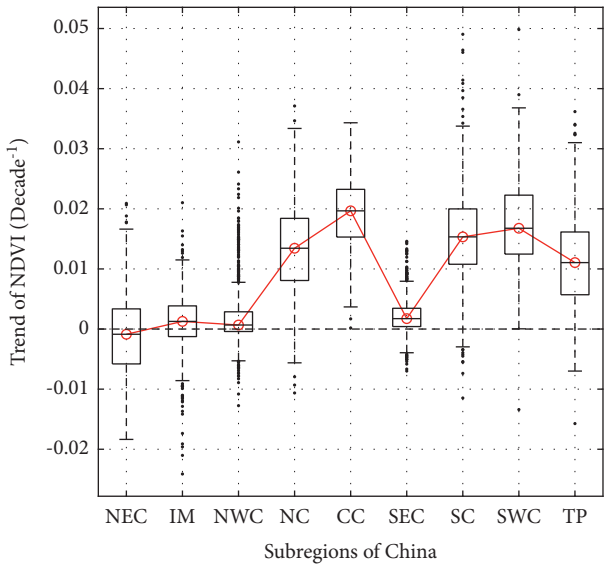

(b)

Figure 2: Continued.

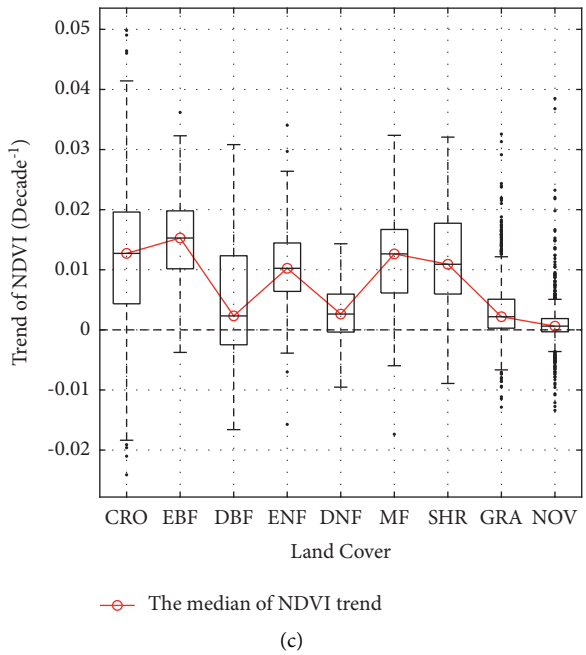

Figure 2: Spatial distribution of change in the annual NDVI (a) in China. The average change in NDVI for each subregion (b) (NEC: Northeast China, IM: Inner Mongolia, NWC: Northwest China, NC: North China, CC: Central China, SEC: Southeast China, SC: South China, SWC: Southwest China, and TP: Tibetan Plateau) and vegetation type (c) (DBF: deciduous broad-leaved forests, DNF: deciduous needleleaf forests, EBF: evergreen broad-leaved forests, CRO: croplands, SHR: shrublands, ENF: evergreen needleleaf forests, MF: mixed forests, and GRA grasslands).

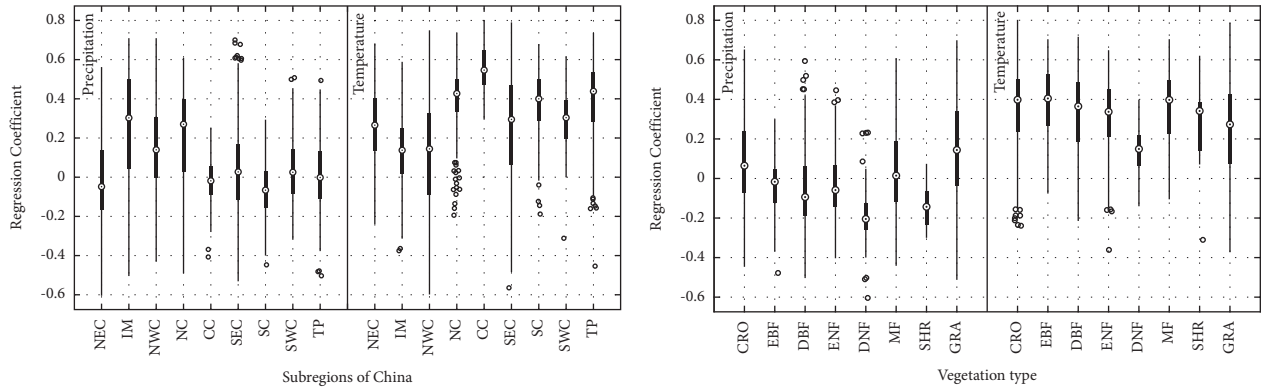

Figure 3: Average regression coefficients of climate variables (precipitation and temperature) for (a) each subregion and (b) vegetation type.

increased in Period 1 (P1), from 1982 to 1998, with a mean annual temperature of 6.66, followed by a dramatic increase after 1998 and decadal warming hiatus early in the 21st century. Period 2 (P2) from 1999 to 2015 was characterized by a higher annual temperature (7.20°C), an intensification of global warming. The MLR model for quantifying the sensitivity of vegetation to climate was also applied to P1 and P2, and then the RESTREND method was used to quantify the contribution of climate changes and human activities in the periods.

The widely used "binning method" was applied to reveal the pattern and characteristics of the vegetation sensitivity to climate changes in different precipitation or temperature conditions. We stratified the annual NDVI data based on the annual precipitation (or air temperature) in bins of 100 mm, from 100 mm for arid region cases to >1700 mm for humid regions (also 2°C bins, from −6°C for sub-frigid regions to 24°C for tropical regions). Here, we focus on each bin greater than 10 grid boxes.

First, we integrated the regression coefficient of temperature (RC_T) and precipitation (RC_P) for each temperature and precipitation bin in P1 (Figure 5(a)–5(c)). In this period, the vegetation growth was more than twice as sensitive to temperature as to precipitation, especially in the bins above 12°C or below 4°C. The negative response to precipitation (RC_P) was found in the bins below 0°C or above

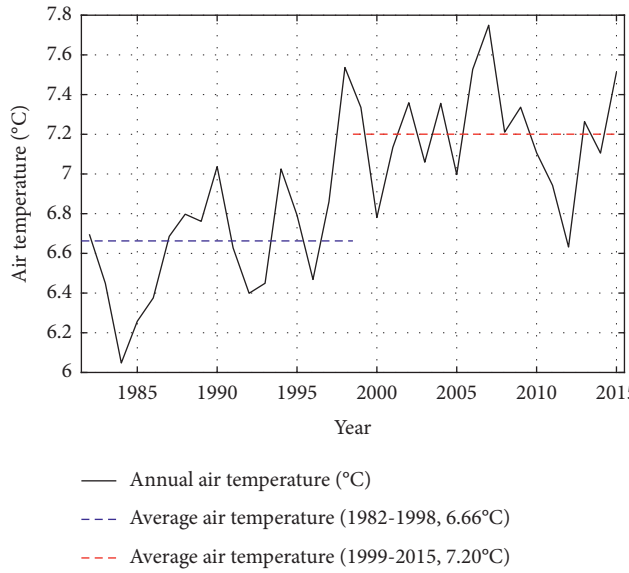

Figure 4: Mean annual air temperature from 1982 to 2015 in China.

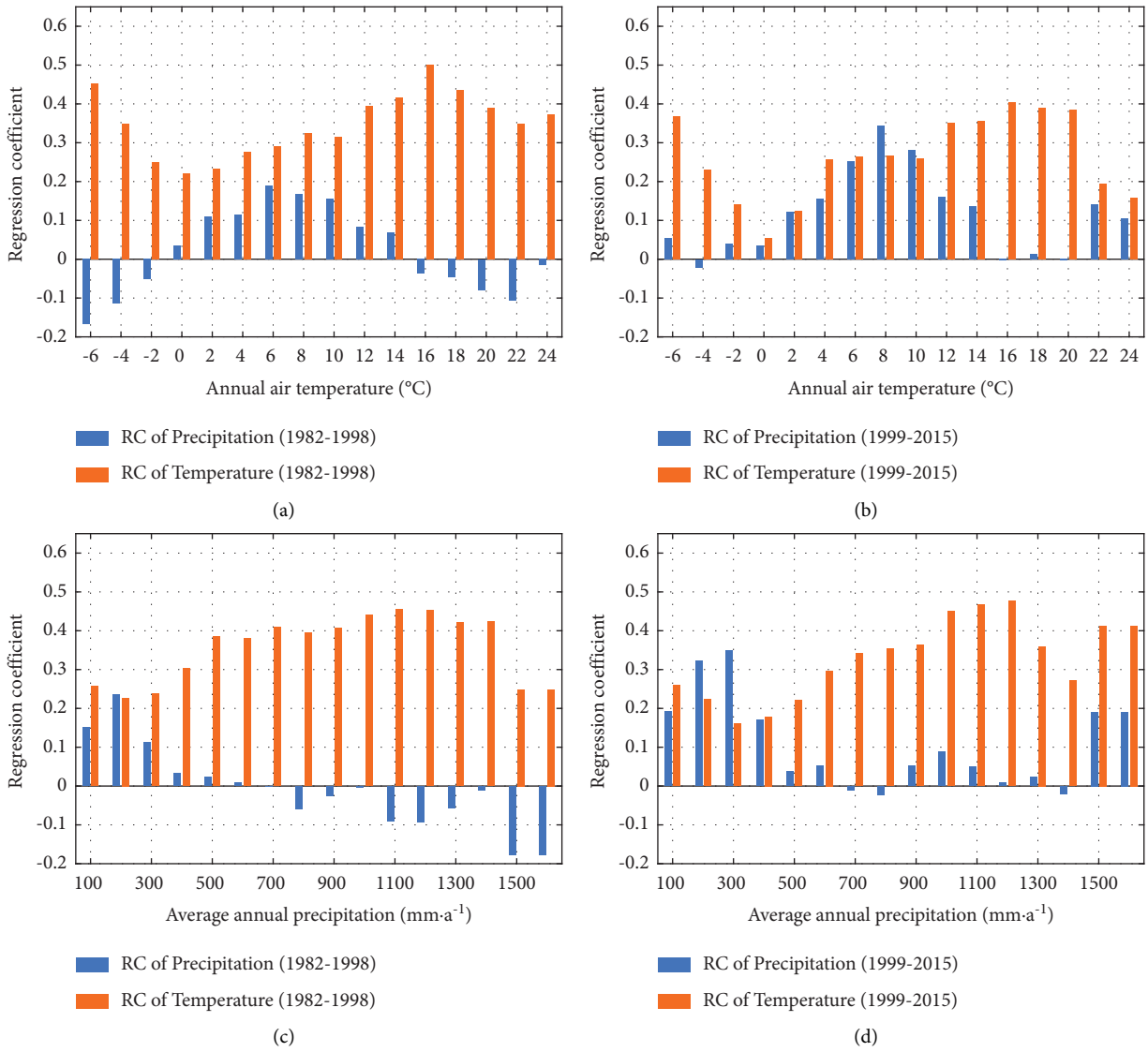

Figure 5: Averaged regression coefficients of precipitation and temperature during the two periods in various bins of ((a) and (b)) annual temperature and ((c) and (d)) annual precipitation.

16°C, and a significant peak occurred between 4°C and 8°C. In this period, RC_P decreases with an increase in precipitation, and the RC_P is larger/less than zero in nonhumid/humid regions (nonhumid/humid regions are the areas where the mean annual precipitation is larger/less than 800 mm). The results indicate that more precipitation could boost vegetation growth in nonhumid regions, whereas excessive precipitation has a negative effect on vegetation growth in humid regions in this period.

We also investigated both RC_T and RC_P for each bin in P2 (Figure 5(b)–5(d)). During this period, there is more sensitivity to precipitation than the temperature in arid/semiarid regions (mean annual precipitation is below 400 mm) or temperate regions (mean annual temperature is more than 8°C and less than 12°C) (Figure 5(b)–5(d)). With global warming, the positive response to precipitation was found in all temperature bins (except for the –4 to –2°C bin). Precipitation is more sensitive than temperature to vegetation growth in some regions, that is, where the mean annual temperature is between 8 and 12°C.

Compared to the probability density function of the correlation coefficient with the mean of 0.408 and standard deviation of 0.168 from 1999 to 2015 (a period of heightened global warming), we found a significantly higher correlation coefficient (CC) with the mean of 0.494 and standard deviation of 0.185 from 1982 to 1998 at the grid box level (Figure 6). The results support that the influence of human activities on vegetation growth became more obvious in the later period. The MLR model, which cannot be explained by climate changes and is usually interpreted as the effects of human activities, increased from 1999 to 2015. Therefore, it is necessary to explore and separate the impact of human activities on vegetation growth using the RESTREND method.

To quantify the influence of human activities on vegetation growth, we define a relative change in the residual trend, which is the ratio of the change in the residual trend in the NDVI to the Long-time average annual NDVI value (defined as $RESTREND_{NDVI}/NDVI$, unit: $(\%)\cdot 10a^{-1}$). The value of relative change in the residual trend ($RESTREND_{NDVI}/NDVI = 1.84\%\cdot 10a^{-1}$) indicates that human activities played a key role in the reversal of land degradation during P1. The spatial distribution of the residual trend showed large regional differences in P1 (Figure 7(a)) with the highest positive values in Central China ($RESTREND_{NDVI}/NDVI = 3.240\%\cdot 10a^{-1}$) and the lowest positive value in Inner Mongolia ($RESTREND_{NDVI}/NDVI = 0.787\%\cdot 10a^{-1}$). Notably, human activities have localized negative effects on vegetation growth in western Inner Mongolia and the Tarim River Basin in western Northwest China in P1.

For P2, the results indicate that the influence of human activities on vegetation is more evident (Figure 7(b)). There was a significant increase in the relative change in the residual trend in the NDVI of all of nine subregions (with the highest positive values in North China, $RESTREND_{NDVI}/NDVI = 6.120\%\cdot 10a^{-1}$), except for Southeast China which had a slight negative effect from human activities on vegetation growth ($RESTREND_{NDVI}/NDVI = -0.299\%\cdot 10a^{-1}$). Interestingly, the brown points

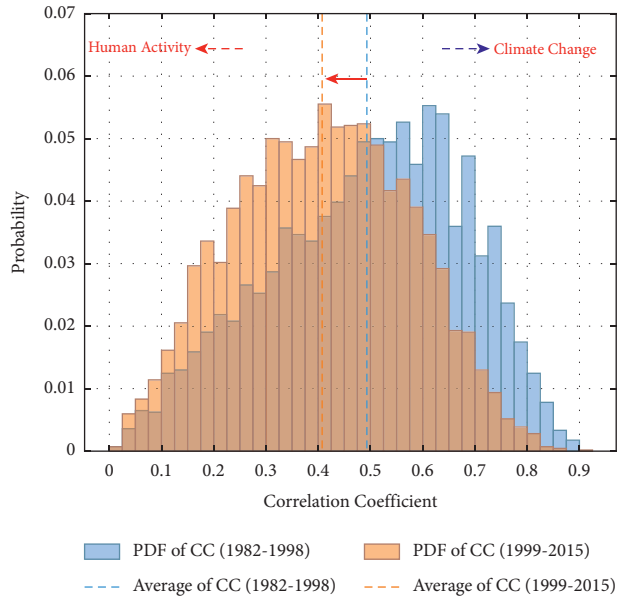

Figure 6: Probability density functions of correlation coefficients using MLR in the two periods.

(degradation in vegetation variation) surrounded by green are the megacities of the Pearl River Delta and Yangtze River Delta in P1 (Figure 7(a)) and the megacities of Chengdu, Xi'an, Zhengzhou, Beijing, Tianjin, Nanjing, Qingdao, and Shanghai in P2 (Figure 7(b)). This suggested that rapid urbanization is one of the causes of vegetation degradation.

5. Discussion

5.1. Climate Changes Sensitivity during the Two Periods. Before the Chinese Grain for Green program was implemented, the vegetation in nonarid areas had a negative response to precipitation as shown in Figures 3 and 5. A more plausible explanation is that temperature and radiation were the limiting factors of vegetation. Precipitation in drought years could satisfy the basic needs for vegetation growth in P1 in semiarid and humid regions of China, because of lower transpiration [39, 40]. With increased vegetation growth and the associated increase in transpiration, the water demand will consequently increase. According to the statistical results from the regression coefficients of multiple linear regression, the sensitivity of vegetation to precipitation increased significantly with vegetation increases in P2. Jiao et al. pointed out that vegetation water constraints are associated with greening trends, which leads to the vegetation becoming increasingly sensitive to precipitation [41]. This finding may explain that the negative regression coefficients of precipitation in P1 shifted to positive coefficients with greening trends in the most subhumid and humid regions in P2.

5.2. The Impacts of Human Activities on Vegetation Change. Previous studies have highlighted that vegetation on the Qinghai-Tibet Plateau has declined significantly due to excessive human interference. Using the RESTREND

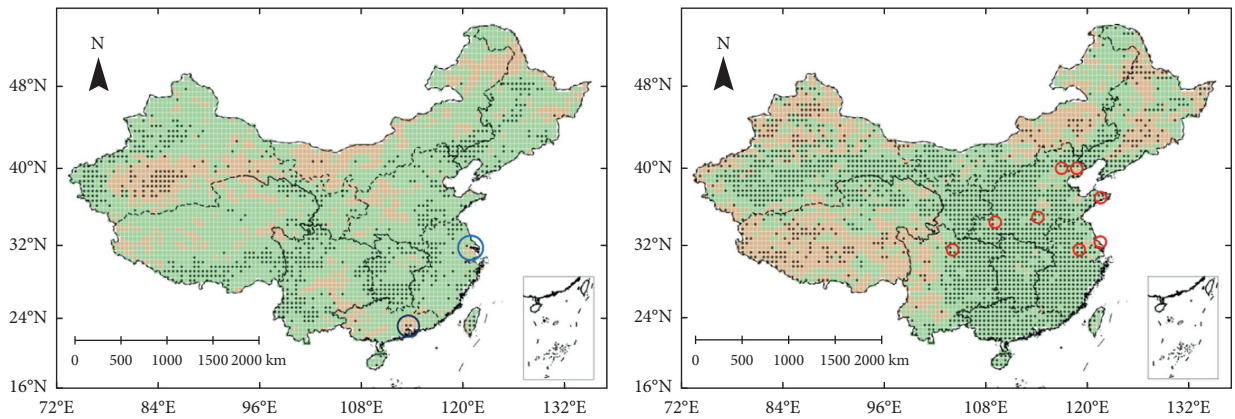

FIGURE 7: Spatial distribution of $RESTREND_{NDVI}$/NDVI during (a) 1982–1998 and (b) 1999–2015 in China. The solid circle denotes a significant ($p < 0.05$) change in $RESTREND_{NDVI}$/NDVI, green (brown) shading indicates an improvement (degradation) in vegetation, the blue circles indicate vegetation degradation areas (1982–1998) in the Pearl River Delta and Yangtze River Delta, and the red circles indicate vegetation degradation areas (1999–2015) in megacities from west to east: Chengdu, Xi'an, Zhengzhou, Beijing, Tianjin, Nanjing, Qingdao, and Shanghai.

method, as shown in Figure 7, we identified the vegetation degradation in P2 [42]. More than 75% of the new cropland has been cultivated at the expense of forest from 1980 to 2000 across the tropical regions. The Grain for Green program induced a considerable reduction in the cultivation of low productivity crops, and any area taken out of cultivation was offset by putting at least an equal additional area into cultivation [43]. The rapid expansion of urbanization is also an important factor leading to vegetation degradation even with the GFG project. One study showed that urban areas increased by $24.6 \times 10^3\,km^2$ (0.26% total area of China), cropland decreased by $4.9 \times 10^3\,km^2$ (0.05% total area of China), and the total area of forest and grassland decreased by $16.4 \times 10^3\,km^2$ (0.17% total area of China) with urbanization from 2000 to 2015 [44]. In this study, the negative effects of urbanization are shown in Figure 7(b), which is in agreement with previous studies [44, 45].

5.3. Limitations and Future Research Directions. Due to the lack of meteorological observation stations in the Qinghai-Tibet Plateau and Northwest China, the global grid meteorological datasets (GPCC and CRU) were used in this study. However, Liang et al. highlighted that a large difference between observation data and global grid data could bias results [46]. This means that the accuracy of the results needs to be further verified using observation datasets. The sensitivities of temperature and precipitation to vegetation growth were quantified at an annual scale. Solar radiation as the energy source of vegetation photosynthesis is also one of the important meteorological elements. Besides, the lag of vegetation response to climate changes should be considered at monthly/seasonal scales [47, 48].

6. Conclusions

In this study, we focus on vegetation responses to climate changes and human activities in various climate areas or land types from two periods (P1, 1982–1998 and P2, 1999–2015) at the grid box level (3839 grid boxes) in China. Nine subregions and nine categorized land covers (vegetation types) were defined. We analyzed the vegetation trends using the NDVI from the whole period of 1982 to 2015. Significant greening trends were detected in most regions, especially in Central China ($Trend_{NDVI} = +0.0190 \cdot 10a^{-1}$), Southwest China ($Trend_{NDVI} = +0.0165 \cdot 10a^{-1}$), and South China ($Trend_{NDVI} = +0.0147 \cdot 10a^{-1}$). Then, we explored the sensitivity of vegetation to climate variables (precipitation and air temperature) using the MLR model. We found that the vegetation is more sensitive to temperature in 70.2% of the areas, and a positive response of vegetation to precipitation was found in nonhumid regions. A binning method was used to reveal the characteristics of the sensitivity of vegetation to climate changes in various climate conditions during the two periods. According to the regression coefficient of the MLR model, the impact of precipitation on vegetation increased significantly in P2 with the intensification of global warming. This indicates that the water demand for vegetation increased significantly in P2.

To separate the impact of climate changes and human activities into the two periods, $RESTREND_{NDVI}$/NDVI was defined as the ratio of the change in the residual trend in the NDVI to the long-time average annual NDVI value as an indicator for quantifying human activities. Human activities play a key role in the reversal of land degradation during P1 ($RESTREND_{NDVI}$/NDVI = $1.840\% \cdot 10a^{-1}$ in P1). The degradation of the Tarim River Basin and eastern Inner Mongolia due to human activities were identified by the RESTREND method. Owing to effective land management, vegetation conditions in most areas of China improved in P2 ($RESTREND_{NDVI}$/NDVI = $2.376\% \cdot 10a^{-1}$). Vegetation degradation, partly caused by overgrazing, was identified in the southern Tibetan Plateau, and vegetation degradation due to urbanization expansion in eight megacities of China was

distinguished. The RESTREND method demonstrates its effectiveness in the quantification of vegetation response to climate changes and human activities.

Data Availability

All data and models used during the study appear in the submitted article.

Conflicts of Interest

The authors declare that there are no conflicts of interest regarding the publication of this article.

Acknowledgments

This work was supported by the National Natural Science Foundation of China (Grant nos. 41901043, 41901362, and 52069006), the Hainan Provincial Natural Science Foundation of China (Grant nos. 420RC601 and 421RC738), and Hainan Province Philosophy and Social Science Planning Base Project (JD(ZC)21-50).

References

[1] Z. Deng, H. Guan, J. Hutson, M. A. Forster, Y. Wang, and C. T. Simmons, "A vegetation-focused soil-plant-atmospheric continuum model to study hydrodynamic soil-plant water relations," *Water Resources Research*, vol. 53, no. 6, pp. 4965–4983, 2017.

[2] G. Forzieri, D. Miralles, P. Ciais et al., "Increased control of vegetation on global terrestrial energy fluxes," *Nature Climate Change*, vol. 10, no. 2, pp. 1–7, 2020.

[3] W. Tao, Q. Wang, L. Guo et al., "An enhanced rainfall-runoff model with coupled canopy interception," *Hydrological Processes*, vol. 34, no. 8, pp. 1837–1853, 2020.

[4] M. Liu, Q. Wang, L. Guo et al., "Influence of canopy and topographic position on soil moisture response to rainfall in a hilly catchment of three Gorges Reservoir area, China," *Journal of Geographical Sciences*, vol. 30, no. 6, pp. 949–968, 2020.

[5] Z. Li, X. Cheng, and H. Han, "Future impacts of land use change on ecosystem services under different scenarios in the ecological conservation area, Beijing, China," *Forests*, vol. 11, no. 5, pp. 584–604, 2020.

[6] J. Zhang, L. Zhou, R. Ma et al., "Influence of soil moisture content and soil and water conservation measures on time to runoff initiation under different rainfall intensities," *Forests*, vol. 182, Article ID 104172, 2019.

[7] M. Borji and A. Samani, "Catchment-scale soil conservation: using climate, vegetation, and topo-hydrological parameters to support decision making and implementation," *The Science of the Total Environment*, vol. 712, no. 3, pp. 136–124, 2019.

[8] S. Chen, Y. Huang, J. Zou, and Y. Shi, "Mean residence time of global topsoil organic carbon depends on temperature, precipitation and soil nitrogen," *Global and Planetary Change*, vol. 100, no. 1, pp. 99–108, 2013.

[9] S. Qu, L. Wang, A. Lin, D. Yu, M. Yuan, and C. Li, "Distinguishing the impacts of climate change and anthropogenic factors on vegetation dynamics in the Yangtze River Basin, China," *Ecological Indicators*, vol. 108, Article ID 105724, 2020.

[10] Q. Zhang, D. Kong, P. Shi, V. P. Singh, and P. Sun, "Vegetation phenology on the Qinghai-Tibetan Plateau and its response to climate change (1982-2013)," *Agricultural and Forest Meteorology*, vol. 248, no. 2, pp. 408–417, 2017.

[11] Z. Zhu, S. Piao, R. B. Myneni et al., "Greening of the earth and its drivers," *Nature Climate Change*, vol. 6, no. 8, pp. 791–795, 2016.

[12] L. Yin, E. Dai, D. Zheng, L. Ma, and M. Tong, "What drives the vegetation dynamics in the Hengduan Mountain region, southwest China: climate change or human activities?" *Ecological Indicators*, vol. 112, Article ID 106013, 2020.

[13] Y. Niu, H. Zhu, S. Yang et al., "Overgrazing leads to soil cracking that later triggers the severe degradation of alpine meadows on the Tibetan Plateau," *Land Degradation & Development*, vol. 30, no. 10, pp. 1243–1257, 2019.

[14] T. Hilker, E. Natsagdorj, R. H. Waring, and A. Wang, "Satellite observed widespread decline in Mongolian grasslands largely due to overgrazing," *Global Change Biology*, vol. 20, no. 2, pp. 418–428, 2014.

[15] G. Li, S. Sun, J. Han et al., "Impacts of Chinese grain for green program and climate change on vegetation in the Loess Plateau during 1982–2015," *The Science of the Total Environment*, vol. 660, pp. 177–187, 2019.

[16] Y. Yuan, T. Zhao, W. Wang, S. Chen, and F. Wu, "Projection of the spatially explicit land use/cover changes in China, 2010–2100," *Advances in Meteorology*, vol. 2013, Article ID 908307, 9 pages, 2013.

[17] W. Yuan, X. Li, S. Liang et al., "Characterization of locations and extents of afforestation from the grain for green project in China," *Remote Sensing*, vol. 5, no. 3, pp. 221-222, 2014.

[18] G. Hou, H. Bi, N. Wang, and Y. Cui, "Optimizing the stand density of robinia pseudoacacia L. forests of the Loess Plateau, China, based on response to soil water and soil nutrient," *Forests*, vol. 10, no. 8, p. 663, 2019.

[19] H. Chen, Z. Huo, X. Dai, S. Ma, X. Xu, and G. Huang, "Impact of agricultural water-saving practices on regional evapotranspiration: the role of groundwater in sustainable agriculture in arid and semi-arid areas," *Agricultural and Forest Meteorology*, vol. 263, pp. 156–168, 2018.

[20] H. Zhang, Q. Zhou, and C. Zhang, "Evaluation of agricultural water-saving effects in the context of water rights trading: an empirical study from China's water rights pilots," *Journal of Cleaner Production*, vol. 313, Article ID 127725, 2021.

[21] Z. Li, X. Sun, Z. Huang et al., "Changes in nutrient balance, environmental effects, and green development after returning farmland to forests: a case study in Ningxia China," *The Science of the Total Environment*, vol. 735, Article ID 139370, 2020.

[22] Q. Guan, L. Yang, N. Pan et al., "Greening and browning of the Hexi Corridor in Northwest China: spatial patterns and responses to climatic variability and anthropogenic drivers," *Remote Sensing*, vol. 10, no. 8, p. 1270, 2018.

[23] Y. Wen, X. Liu, J. Yang, K. Lin, and G. Du, "NDVI indicated inter-seasonal non-uniform time-lag responses of terrestrial vegetation growth to daily maximum and minimum temperature," *Global and Planetary Change*, vol. 177, pp. 27–38, 2019.

[24] M. Jiang, S. Tian, Z. Zheng, Q. Zhan, and Y. He, "Human activities influences on vegetation cover changes in Beijing, China from 2000 to 2015," *Remote Sensing*, vol. 9, no. 3, p. 271, 2017.

[25] H. Wang, G. Liu, Z. Li, P. Wang, and Z. Wang, "Comparative assessment of vegetation dynamics under the influence of climate change and human activities in five ecologically

vulnerable regions of China from 2000 to 2015," *Forests*, vol. 10, no. 4, p. 317, 2019.

[26] A. AghaKouchak, A. Farahmand, F. S. Melton et al., "Remote sensing of drought: progress, challenges, and opportunities," *Reviews of Geophysics*, vol. 53, pp. 452–480, 2015.

[27] M. Schultz, J. Voss, M. Auer, S. Carter, and A. Zipf, "Open land cover from OpenStreetMap and remote sensing," *International Journal of Applied Earth Observation and Geoinformation*, vol. 63, pp. 206–213, 2017.

[28] N. Levin, C. C. M. Kyba, Q. Zhang et al., "Remote sensing of night lights: a review and an outlook for the future[J]," *Remote Sensing of Environment*, vol. 237, Article ID 111443, 2020.

[29] Y. Yi, B. Wang, M. Shi, and Z. Meng, "Variation in vegetation and its driving force in the middle reaches of the Yangtze River in China," *Water*, vol. 13, p. 2036, 2021.

[30] Z. Jiang, A. R. Huete, K. Didan, and T. DMiura, "Development of a two-band enhanced vegetation index without a blue band," *Remote Sensing of Environment*, vol. 112, no. 10, pp. 3833–3845, 2008.

[31] F. Tian, Y. H. Lü, B. J. Fu et al., "Challenge of vegetation greening on water resources sustainability: insights from a modeling-based analysis in Northwest China," *Hydrological Processes*, vol. 31, no. 7, pp. 1469–1478, 2017.

[32] L. Guo, F. Sun, W. Liu et al., "Response of ecosystem water use efficiency to drought over China during 1982–2015: spatiotemporal variability and resilience," *Forests*, vol. 10, no. 7, p. 598, 2019.

[33] F. Pei, Y. Zhou, and Y. Xia, "Application of normalized difference vegetation index (NDVI) for the detection of extreme precipitation change," *Forests*, vol. 12, no. 5, p. 594, 2021.

[34] W. Ge, L. Deng, F. Wang, and J. Han, "Quantifying the contributions of human activities and climate change to vegetation net primary productivity dynamics in China from 2001 to 2016," *Science of the Total Environment*, vol. 773, Article ID 145648, 2021.

[35] S. Piao, J. Tan, A. Chen et al., "Leaf onset in the northern hemisphere triggered by daytime temperature," *Nature Communications*, vol. 6, no. 1, pp. 1–8, 2015.

[36] K. H. Hamed and A. R. Rao, "A modified Mann-Kendall trend test for auto correlated data," *Journal of Hydrology*, vol. 204, no. 1-4, pp. 182–196, 1998.

[37] H. Wang, G. Liu, Z. Li, P. Wang, and Z. Wang, "Assessing the driving forces in vegetation dynamics using net primary productivity as the indicator: a case study in Jinghe River Basin in the Loess Plateau," *Forests*, vol. 9, no. 7, p. 374, 2018.

[38] C. Qian, L. Shao, X. Hou, B. Zhang, W. Chen, and X. Xia, "Detection and attribution of vegetation greening trend across distinct local landscapes under China's grain to green program: a case study in Shaanxi Province," *Catena*, vol. 183, Article ID 104182, 2019.

[39] Y. Chen, K. Wang, and Y. Lin, "Balancing green and grain trade," *Nature Geoscience*, vol. 8, pp. 739–741, 2015.

[40] X. Feng, B. Fu, S. Piao et al., "Revegetation in China Loess Plateau is approaching sustainable water resource limits," *Nature Climate Change*, vol. 6, no. 11, 2016.

[41] W. Jiao, L. Wang, W. K. Smith, Q. Chang, H. Wang, and P. D'Odorico, "Observed increasing water constraint on vegetation growth over the last three decades," *Nature Communications*, vol. 12, p. 3777, 2021.

[42] R. B. Harris, "Rangeland degradation on the Qinghai-Tibetan plateau: a review of the evidence of its magnitude and causes," *Journal of Arid Environments*, vol. 74, pp. 1–12, 2010.

[43] X. Liu, C. Zhao, and W. Song, "Review of the evolution of cultivated land protection policies in the period following China's reform and liberalization," *Land Use Policy*, vol. 67, pp. 660–669, 2017.

[44] J. Ning, J. Liu, W. Kuang et al., "Spatiotemporal patterns and characteristics of land-use change in China during 2010–2015," *Journal of Geographical Sciences*, vol. 28, pp. 547–562, 2018.

[45] D. Li, S. Wu, Z. Liang, and S. Li, "The impacts of urbanization and climate change on urban vegetation dynamics in China," *Urban Forestry & Urban Greening*, vol. 54, Article ID 126764, 2020.

[46] C. Liang, T. Shi, X. Wei et al., "Drying and wetting trends and vegetation covariations in the drylands of China," *Water*, vol. 12, p. 933, 2020.

[47] L. Hua, H. Wang, H. Sui, W. Brian, H. Michael, and W. Jianxun, "Mapping the spatial-temporal dynamics of vegetation response lag to drought in a semi-arid region," *Remote Sensing*, vol. 11, p. 1873, 2019.

[48] L. Ji and A. J. Peters, "Assessing vegetation response to drought in the northern Great Plains using vegetation and drought indices," *Remote Sensing of Environment*, vol. 87, pp. 85–98, 2003.